LASER-ASSISTED SURFACE MODIFICATION OF ZIRCONIA-BASED MATERIALS TO GUIDE OSTEOBLAST RESPONSES FOR DENTAL APPLICATIONS

***N. Garcia de Albeniz Lopez de Aberatsuri*[1,2], *J.J. Roa Rovira*[1], *C. Mas Moruno*[2]**

[1] Center for Structural Integrity, Reliability and Micromechanics of Materials (CIEFMA), Department of Materials Science and Engineering, Universitat Politècnica de Catalunya, 08019 Barcelona, Spain
[2] Biomaterials, Biomechanics and Tissue Engineering Group (BBT), Department of Materials Science and Engineering, Universitat Politècnica de Catalunya, 08019 Barcelona, Spain

The project is aimed at investigating the effect of laser surface modification of dental-grade zirconia (3Y-TZP) to guide cellular behaviour. A nanosecond laser was employed to fabricate groove patterns on the surface of 3Y-TZP, yielding three different topographies according to the groove periodicity (30, 50 and 100µm). The resulting topography, microstructure, hardness and hydrothermal degradation resistance of the modified zirconia was assessed by means of advanced characterization techniques. A cellular study was conducted to evaluate the behaviour of human mesenchymal stem cells on the patterned samples in term of adhesion and cell morphology. The results showed grooves of approximately 1.7µm heigh with pronounced pile-up due to the melting and re-solidification of the material. The phase analysis revealed that no phase transformation is induced during the laser modification; however, a non-homogeneous monoclinic phase distribution was observed on the patterned surfaces after hydrothermal degradation. Finally, all the patterned surfaces allowed cell attachment, increased cell area and favoured cell elongation and alignment in the direction of the laser patterns.

Keywords: zirconia, laser patterning, topography, phase transformation, hydrothermal degradation, cell adhesion

1. INTRODUCTION

At present, zirconia-based materials are gaining interest in implant applications due to their superior biocompatibility, reduced bacterial plaque affinity, and lower corrosion when compared to traditional titanium implants, and higher fracture toughness and superior strength over other advanced ceramic materials [1].
In terms of biological success of the implant, it is of vital importance to achieve a strong and durable integration between the bone and the implant surface in order to guarantee the long-term durability of the material under service-like working conditions [2]. In this regard, it is well known that the osseointegration process depends on the surface characteristics of the implant, from which the surface topography (e.g., roughness) is considered to be a key feature. Hence, various surface modification approaches have been investigated to modify the surface properties of zirconia to enhance its biological performance (e.g., grinding, sandblasting, acid etching, laser treatment, etc.). Among those, laser texturing is considered to be an advantageous technique since it can produce defined micro-patterns (grids, grooves, pits, etc.) in a fast and accurate way and with high repeatability [3]. Nevertheless, ceramic materials are sensitive to any surface alteration, meaning that the changes produced during the laser modification may influence the mechanical properties, and in the particular case of zirconia, can also promote the ageing phenomenon [4]. Thus, new studies addressing both the biological performance and the mechanical integrity of zirconia are needed. In this regard, the main objective of this study is to evaluate the effect of nanosecond laser modification o zirconia on the topography, phase stability, hydrothermal degradation, and cell behaviour.

2. EXPERIMENTAL PROCEDURE

2.1. Sample preparation

Commercially available zirconia powder stabilized with 3 mol% yttria (TZ-3YSB-E, Tosoh) was used to produce 15mm diameter disc-shaped specimens. The samples were shaped by cold isostatic pressing at 288MPa and then the green bodies were sintered in air at 1450ºC for two hours with heating and cooling rates of 6°C/min. Posteriorly, the surfaces of all the discs were grounded, then mirror-like polished by using diamond suspensions of decreasing particle size (30–6–3µm), and a finalizing step of 0.02µm particle size alumina polishing was done.

2.2. Laser patterning

The surface patterning was carried out using the Spectra-Physics Explorer One 349-120 laser source operating at 349nm wavelength, <5 ns pulse duration, and up 120 µJ energy per pulse. A Design of Experiment (DoE) was planned to find out the optimum combination of the laser parameters (intensity, scan speed and frequency) that allows to obtain the desired pattern: a peak-valley height in the range of 1-2µm and minimize the pile-up effect. After the topographical characterization of the DoE via Atomic Force Microscopy (AFM), Laser Scanning Confocal microscopy (LSCM) and Contact Profilometry, the selected laser parameters were a laser intensity of 2.5A, 500Hz output frequency, and 2bit/ms scan speed. All the samples were treated with a single pulse.
The patterns produced on the zirconia surface consisted on parallel grooves with different peak-to-peak distance (periodicity). Concretely, 30µm, 50µm and 100µm periodicities were chosen for the study (denoted as 30, 50, and 100, respectively), and mirror-like polished zirconia was also included as a reference (ref).

2.3. Surface characterization

A Laser Scanning Confocal Microscope (LSCM, Olympus Lext OLS3100) was used for the topographical observation and to obtain the roughness parameters.

X-Ray Diffraction (XRD) was used to evaluate the crystalline phases of the samples before and after the hydrothermal degradation. XRD spectra were recorded on a diffractometer (D8-Advance, Bruker) using Cu Kα radiation (40 kV and 30 mA) in an angle range of $20° \leq 2\theta \leq 70°$ at a scan rate of 1 s/step and a scan size of 0.02°. The monoclinic volume fraction (V_m) was estimated by the equation proposed by Toraya *et al.* [5]

$$V_m = \frac{1.311\,[Im(\bar{1}11) + Im(111)]}{1.311\,[Im(\bar{1}11) + Im(111)] + It(101)} \quad (1)$$

where I_m and I_t correspond to the intensities of the monoclinic and tetragonal peaks, respectively.

Confocal micro-Raman Spectroscopy technique was used to analyse the m-phase distribution along the patterns (along the laser treated and non-treated zones). An area of 30x50µm was selected for the study and the volume fraction of the monoclinic phase (V_m) was calculated by the equation proposed by Katagiri *et al.* [6]:

$$V_m = \frac{I_m^{181} + I_m^{190}}{2.2\,(I_t^{247}) + I_m^{181} + I_m^{190}} \quad (2)$$

where I_m and I_t correspond to the integrated intensities of the monoclinic and tetragonal bands, respectively.

2.4. Mechanical characterization

The Akashi MVK-H0 durometer was used to determine the Vickers hardness (HV) of all the zirconia samples before and after hydrothermal degradation. A load of 10kgf was applied and five indentations were done for each sample type in order to get statistical signification.

2.4. Hydrothermal degradation

Accelerated degradation tests in water steam were performed at 134 °C and 2 bars of pressure (Micro8, Selecta). The samples were degraded for 10h.

2.5. Cell adhesion study

Human mesenchymal stem cells (hMSCs) at passage 6 were cultured in Advanced Dulbecco's Modified Eagle's Medium (DMEM) supplemented with 10% (v/v) fetal bovine serum (FBS), 50 U/mL penicillin, 50 U/mL streptomycin and 1% (w/v) L-glutamine and maintained at 37ºC in a humidified 5% CO_2 atmosphere. When the flask reached an 80% confluence, the hMSCs were detached with trypsin-EDTA and seeded at a concentration of 5000 cells/sample in the same culture medium. After 6 hours, the medium was aspired and the adhered cells were fixed paraformaldehyde (PFA, 4 % w/v in PBS) for 30 min and stored at 4ºC in PBS.

For morphology assessment, via fluorescence staining, the cells were permeabilized with 0.05% (w/v) Triton X-100 in PBS for 20 min followed by a 30 min blocking step with bovine serum albumin (BSA, 1 % (w/v) in PBS). Then the focal adhesions were stained with mouse anti-vinculin (1:100, in BSA 1 %, 1h), the actin filament were stained using Alexa Fluor 488 (2drops/ml)-conjugated phalloidin (1:400, in triton 0.05%, 1h), and the nuclei was stained with 4′,6-diamidino-2-phenylindole (DAPI) (1:1000, in PBS-glycine 20 mM) for 2 min. A fluorescence LSCM was used to examine the samples and Fiji/Image-J package for image analysis.

3. RESULTS AND DISCUSSION

3.1. Topographical characterization

As depicted in the LSCM images of **Figure 1,** the laser modification allowed the patterning of grooved surfaces of different periodicities (30, 50 and 100). These topographies are characterized by a laser trace (dark grey) and a non-treated zone (light grey) that decreases as the periodicity becomes smaller, been almost inestimable in the 30 sample (**Figure 1a**). Moreover, the images revealed a micrometer roughness (the valley and pile-up), but also nanoscale roughness along the valleys.

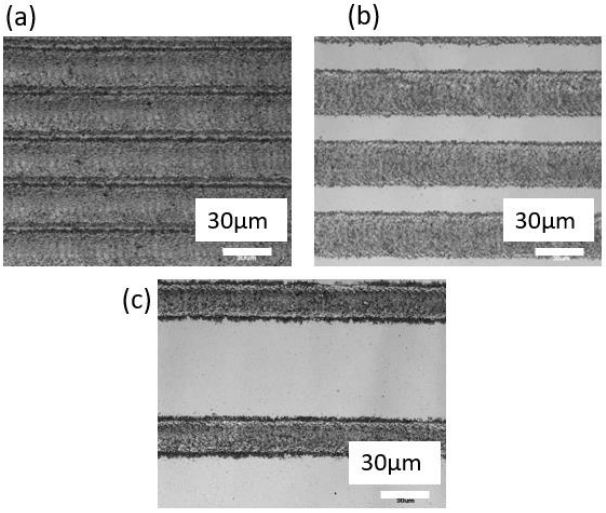

Figure 1. LSCM Topographical images of the samples after laser treatment. Groove periodicity: (a)30 (b)50 and (c) 100.

The total height (Ht) measured in the three patterned samples is within the desired range for the cellular study (between 1-2µm). However, almost 1/3 of the total height is due to the pile-up generated with the laser beam as a side effect. Similarly, the pile-up width measured is half of the total width of the laser path: ~ 14µm of pileup (~7µm on each side) compared with ~30µm of total width. Ideally, the pile-up was intended to be the minimum as possible, since it may decrease the mechanical properties of the material and promote the t→m phase transformation. Compared with other studies where laser surface modification of zirconia have been performed, the side effect produced in this work is much higher [7], [8]. This is attributed to the accuracy of the laser used in our study (i.e. nanosecond laser), compared to the use of pico- or femto-second laser, which are more accurate.

Table 1. Topography analysis performed by the LCSM (x50). H_v, H_p, and H_t, indicate valley, pile-up, and total height (respectively); and W_v, W_p, and W_t, indicate valley, pile-up, and total width (respectively). All the measures are in µm.

	H_v	H_p	H_t	W_v	W_p	W_t
30	1.19 *±0.12*	0.64 *±0.10*	1.75 *±0.15*	14.66 *±1.12*	6.42 *±0.78*	26.20 *±0.99*
50	1.08 ±0.18	0.60 *±0.15*	1.64 *±0.21*	15.00 *±1.98*	7.51 *±1.34*	30.60 *±2.47*
100	1.23 *±0.14*	0.64 *±0.13*	1.81 *±0.16*	13.38 *±0.74*	7.33 *±0.95*	29.44 *±1.64*

3.2. Hydrothermal degradation

3.2.2. X-ray diffraction

Figure 2 shows the V_m calculated from the XRD analysis. The m-phase content was negligible in the non-degraded samples (black line) since it was lower that 2% in all cases. However, after 10 hours of degradation in steam water, the t-→m- phase transformation was triggered in the four specimens (in blue). The $V_m(\%)$ of the degrades samples ranged from 25% (100um) to 45% (30um).

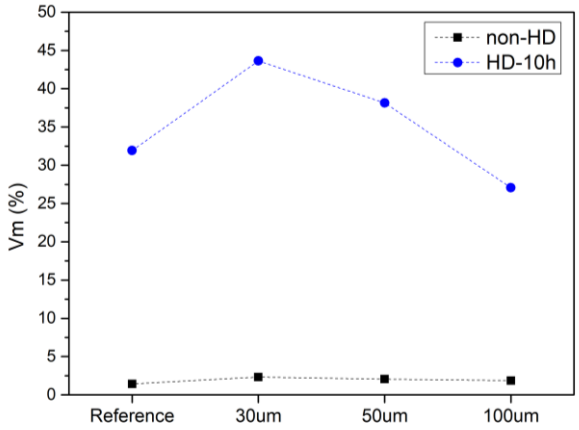

Figure 2. Monoclinic volume fraction calculated from the XRD of the samples before (black dots) and after LTD (blue dots).

3.2.1. Raman spectroscopy

Raman spectroscopy data is in accordance with the XRD results. It can be seen that the polished zirconia (**Figure 3a**) and the laser modified samples (**Figure 3b** to **d**) did not present any m-phase content before the hydrothermal degradation process. By contrast, after 10 hours in steam water, all the samples present t-→m-phase transformation on the surface (**Figure 3e** to **f**). According to the Raman calculation, the V_m varies from 15 - 90% depending of the sample type and surface spot. Among all the samples, the 30 periodic pattern displayed the worst low thermal degradation (LTD) resistance presenting a V_m ranging from 50% to 90% along all the examined surface (**Figure 3f**). However, it must be noted that the V_m estimated from the Raman spectra differs from the XRD results. This is because the laser of the Raman penetrates up to 40µm, leading to Raman signals collected from well below the surface layer and resulting in an inaccurate estimation [9]. On the contrary, in the XRD analysis the 63% of the attenuated signal comes from depths less than 2µm and the 95% from depths up to 5µm, [10]. Thus, the V_m calculated from the XRD analysis may be more representative.

Moreover, the Raman spectra mapping evidenced that there is a non-homogeneous distribution of the m-phase distribution along the surface of the aged and patterned 3Y-TZP samples. In particular, three spots were differentiated, as indicated in **Figure 3g**: the non-modified part, the laser valley zone, and the pileup, which is the most transformed zone in all cases (**Figure 3f** to **h**). From the Raman analysis it can be stated that the 50µm sample (**Figure 3g**) presented the highest aging resistance since its non-treated part showed even less V_m than the control.

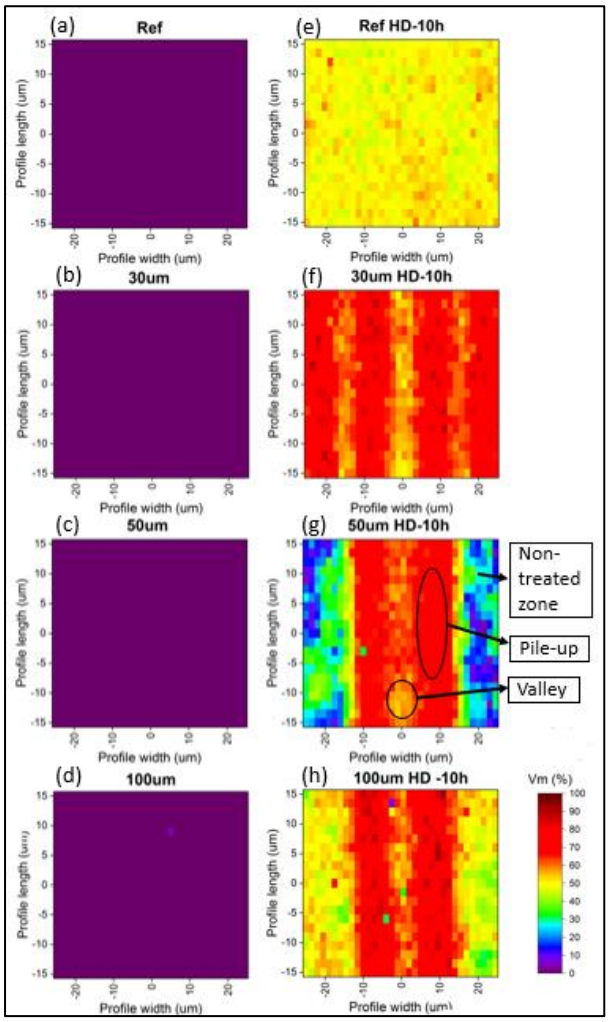

Figure 3. Raman spectroscopy of the samples before (a, b, c, d) and after 10 hours in water steam (e, f, g, h).

3.2.2. Vickers Hardness

Vickers Hardness (HV) of the four sample types before and after LTD was measured as an indicative of how the mechanical properties are affected by the laser patterning and the hydrothermal degradation. In **Table 1** it can be observed that surface modification itself did not influence the hardness of the zirconia since there is no significative change between the measured values. In contrast, after accelerated aging a drop in the hardness was observed in all the specimens, which may be related with the phase transformation that has been already described on the aged zirconia. Among all the samples, the 30 sample had the higher HV, which may indicate that laser-mediated pileup acts as a hardening mechanism.

Table 2. Vickers hardness (HV) before and after LTD.

	Before LTD	**After LTD**
Ref	13.92 ± *0.20*	13.44 ± *0.14*
30	14.04 ± *0.45*	13.73 ± *0.20*
50	13.90 ± *0.20*	13.18 ± *0.26*
100	13.88 ± *0.32*	13.03 ± *0.26*

3.3. Cellular study

The fluorescence LCSM images (**Figure 4a** to **d**) showed that all the examined surfaces allowed cell attachment, which in the case of 50 (**Figure 4c**) and 100 samples (**Figure 4d**) was found to be higher than on the polished specimen. Furthermore, the cells adhering onto these two

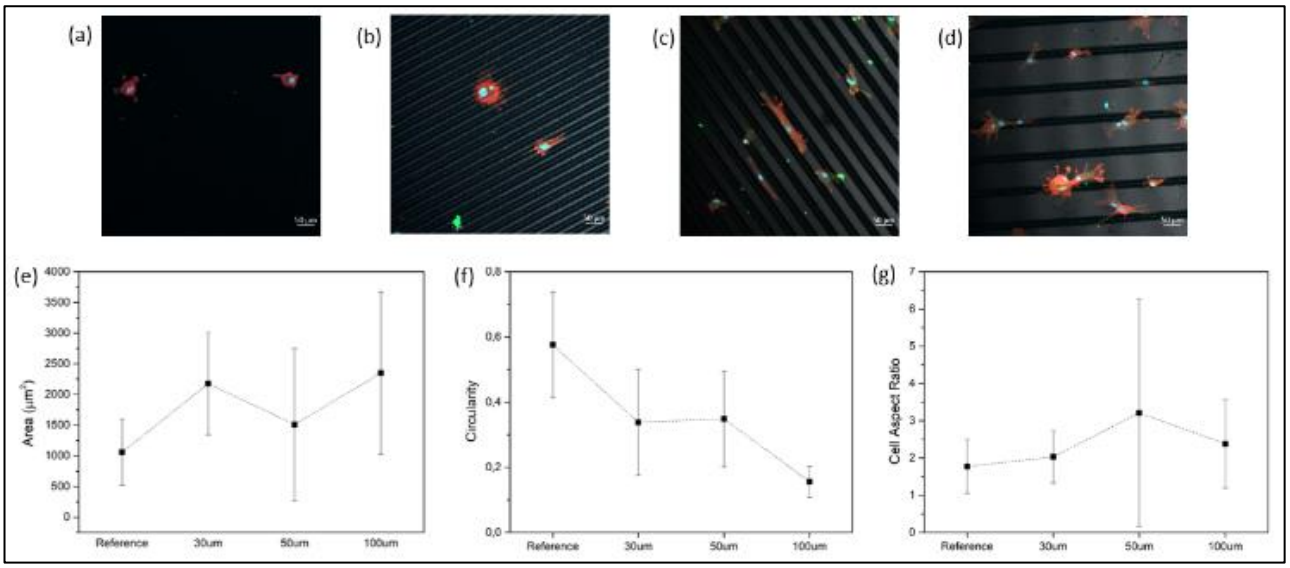

Figure 4. hMSCs adhesion result after 6h of incubation. Fluorescence LCSM images of the cells cultured on reference (a), and 30 (b), 50 (c), and 100 (d) patterned zirconia samples. Note in the images: actin filaments in red(red), cell nuclei in blue(blue), and focal adhesion in green. Also, the cell area (µm2) (a), cell circularity (b), and cell aspect ratio (b) have been calculated from the images

samples displayed a more elongated shape and cytoskeletal elongations that may favour cell anchorage to the surfaces, indicating a stronger adhesion to these topographies.

The quantitative analysis of cell morphology revealed that the laser patterns increased the cell area as compared to polished 3Y-TZP (ref) (**Figure 4e**). In detail, the average cell area was doubled on the 30 and 100 samples, and increased by a factor of 1,5 on the 50 specimen. The cell morphology was further characterized by analysing the circularity (from 0-1, being 1 the maximum circularity) and aspect ratio (level of cell elongation) of the cells. The circularity is related with the cell perimeter and it indicates whether the cell has a rounded shape or not. A decrease in cell circularity was observed on the laser modified samples in contrast with the reference specimens (**Figure 4f**), indicating a more elongated/branched morphology, i.e. less rounded cells, as initially observed in the fluorescence images. More specifically, the cells adhered to the 100 sample displayed the lowest circularity. Moreover, the aspect ratio values shown in **Figure 4g** indicate a slight tendency towards increased cell elongation on the laser-patterned samples compared to the reference. In this case, the cells attached to the 50µm pattern presented the most pronounced elongation, almost two times higher than the reference. The high standard deviation of these results suggests some extent of variability in the cellular responses, but on the whole clearly indicate that the topographies are able to influence cell adhesion and morphology on the surfaces.

4. CONCLUSIONS

The micropatterning of dental zirconia was successfully achieved by nanosecond laser micromachining. The modified surfaces consisted on grooved topographies of variable periodicity (30, 50, 100µm), in which a significative pile-up was generated, but any phase transformation was observed. Furthermore, the laser treatment did no significantly influence the LTD resistance when compared to non-treated 3Y-TZP, and the m-phase was found to be non-homogeneously distributed along the patterned surfaces. Finally, from the cellular study it can be concluded that the adhesion of the hMSCs is increased by the topographical changes on the laser-modified specimens. Furthermore, the patterned specimens favoured cell spreading, cytoskeletal elongations, and alignment, which is expected to positively influence cell behaviour in terms of proliferation, migration and differentiation. Nonetheless, a deeper characterization is required to select the laser pattern that promotes the best cellular response.

5. REFERENCES

[1] A. A. Madfa, F. A. Al-Sanabani, N. H. Al-Qudami, J. S. Al-Sanabani, and A. G. Amran, "Use of Zirconia in Dentistry: An Overview," *Open Biomater. J.*, vol. 5, no. 1, pp. 1–9, 2014.

[2] C. Mas-Moruno, B. Su, and M. J. Dalby, "Multifunctional Coatings and Nanotopographies: Toward Cell Instructive and Antibacterial Implants," *Adv. Healthc. Mater.*, vol. 8, no. 1, 2019.

[3] J. Han, F. Zhang, B. Van Meerbeek, J. Vleugels, A. Braem, and S. Castagne, "Laser surface texturing of zirconia-based ceramics for dental applications: A review," *Mater. Sci. Eng. C*, vol. 123, no. March, p. 112034, 2021.

[4] E. Roitero, M. Ochoa, M. Anglada, F. Mücklich, and E. Jiménez-Piqué, "Low temperature degradation of laser patterned 3Y-TZP: Enhancement of resistance after thermal treatment," *J. Eur. Ceram. Soc.*, vol. 38, no. 4, pp. 1742–1749, 2018.

[5] H. Toraya, M. Yoshimura, and S. Somiya, "Calibration Curve for Quantitative Analysis of the Monoclinic-Tetragonal ZrO2 System by X-Ray Diffraction," *J. Am. Ceram. Soc.*, vol. 67, no. 6, p. 119-121, 1984.

[6] G. Katagiri, H. Ishida, A. Ishitani, and T. Masaki, "Direct determination by a Raman microprobe of the transformation zone size in Y2O3 containing tetragonal ZrO2 polycrystals.," *Adv. Ceram.*, vol. 24A, pp. 537–544, 1988.

[7] A. Carvalho, L. Cangueiro, V. Oliveira, R. Vilar, M. H. Fernandes, and F. J. Monteiro, "Femtosecond laser microstructured Alumina toughened Zirconia: A new strategy to improve osteogenic differentiation of hMSCs," *Appl. Surf. Sci.*, vol. 435, pp. 1237–1245, 2018.

[8] E. Roitero, F. Lasserre, M. Anglada, F. Mücklich, and E. Jiménez-Piqué, "A parametric study of laser interference surface patterning of dental zirconia: Effects of laser parameters on topography and surface quality," *Dent. Mater.*, vol. 33, no. 1, pp. e28–e38, 2017.

[9] A. Paul, B. Vaidhyanathan, and J. Binner, "Micro-Raman spectroscopy of indentation induced phase transformation in nanozirconia ceramics," *Adv. Appl. Ceram.*, vol. 110, no. 2, pp. 114–119, 2011.

[10] J. A. Muñoz-Tabares, "Cambios microestructurales en 3Y-TZP desbastada y su influencia en la degradación hidrotérmica," Universidad Politécnica de Cataluña, 2010.